Theoretical Study of the Adsorption and Dissociation of Oxygen on Pt(111) in the Presence of Homogeneous Electric Fields

Matthew P. Hyman and J. Will Medlin*

Department of Chemical and Biological Engineering, University of Colorado, Boulder, Colorado 80309

Received: October 24, 2004; In Final Form: December 12, 2004

The effect of homogeneous electric fields on the adsorption energies of atomic and molecular oxygen and the dissociation activation energy of molecular oxygen on Pt(111) were studied by density functional theory (DFT). Positive electric fields, corresponding to positively charged surfaces, reduce the adsorption energies of the oxygen species on Pt(111), whereas negative fields increase the adsorption energies. The magnitude of the energy change for a given field is primarily determined by the static surface dipole moment induced by adsorption. On 10-atom Pt(111) clusters, the adsorption energy of atomic oxygen decreased by ca. 0.25 eV in the presence of a 0.51 V/Å (0.01 au) electric field. This energy change, however, is heavily dependent on the number of atoms in the Pt(111) cluster, as the static dipole moment decreases with cluster size. Similar calculations with periodic slab models revealed a change in energy smaller by roughly an order of magnitude relative to the 10-atom cluster results. Calculations with adsorbed molecular oxygen and its transition state for dissociation showed similar behavior. Additionally, substrate relaxation in periodic slab models lowers the static dipole moment and, therefore, the effect of electric field on binding energy. The results presented in this paper indicate that the electrostatic effect of electric fields at fuel cell cathodes may be sufficiently large to influence the oxygen reduction reaction kinetics by increasing the activation energy for dissociation.

Introduction

The interaction of oxygen with platinum surfaces in a vacuum has been extensively studied by theoretical[1−5] and experimental techniques such as electron energy loss spectroscopy (EELS),[6−8] molecular beam studies,[8,9] near-edge X-ray absorption fine structure spectroscopy (NEXAFS),[10,11] photoemission spectroscopy,[6,12] and temperature-programmed desorption (TPD).[13−16] Additionally, the reaction of hydrogen and oxygen catalyzed by platinum has been extensively studied, primarily due to its importance in automotive catalysis.[17−31] However, the mechanism for the oxygen reduction reaction in an electrochemical environment, as it occurs at fuel cell cathodes, is not well understood. The lack of mechanistic knowledge creates difficulties in determining reasons for the improved performance of certain Pt-alloy catalysts and in designing new catalysts for more efficient fuel cell operation.[32−34] The electric double layer (EDL) present at the metal/solution interface in electrochemical cells may have a profound influence on the interaction of oxygen with the Pt catalysts typically used as fuel cell cathodes, but this influence has not been well-studied. The main reason for this lack of mechanistic information is that EDL physics are not accounted for by the vacuum techniques described above. The lack of in situ spectroscopic techniques able to identify reaction intermediates leaves electrochemical methods such as the rotating disk electrode[35,36] and kinetic isotope experiments[37,38] as the only sources of experimental data for indirect mechanism development.

The motivation for this work stems from the need to understand the difference between electrochemical and nonelectrochemical environments at the atomic level. The nonelectrochemical oxygen reduction reaction is reasonably well understood. Briefly, oxygen from the gas phase molecularly adsorbs on the Pt(111) surface in both magnetic and nonmagnetic states and dissociates above ca. 150 K, with atomic oxygen attaining a p(2 × 2) surface pattern at maximum coverage.[2,7−9,14−16] Previous work suggests that although the two molecular precursor states are nearly energetically degenerate, the nonmagnetic state is the immediate dissociation precursor.[3,8] After dissociation, atomic oxygen reacts with atomic hydrogen via two distinct pathways. Above the desorption temperature of water, atomic hydrogen sequentially combines with atomic oxygen on Pt(111) to form water, which then desorbs from the surface.[17,26,27] Below the desorption temperature, water actively participates in the reaction, reacting with atomic oxygen to form hydroxyl radicals.[19,23,24] In both pathways, molecular oxygen dissociation is the first step leading to water formation.

In electrochemical environments, mechanistic studies have yielded conflicting results regarding the reaction pathway for O_2 reduction. Kinetic isotope studies indicate that molecular oxygen dissociates immediately following adsorption in electrochemical environments,[37,38] but rotating disk electrode studies[35,36] and theoretical studies employing one or two metal atoms to approximate the metal surface[39−41] suggest that charge transfer precedes dissociation and is rate-limiting. These conflicting results have hindered the ability to understand the reaction mechanism. Thus, the overall goal of our work is to determine how the presence of an EDL at the metal/solution interface alters the well-understood interaction of O_2 with Pt surfaces in a vacuum. If the mechanism for O_2 dissociation is substantially affected by EDL-like physics, it may be possible to rationalize the relatively slow kinetics of oxygen reduction at fuel cell cathodes and to identify changes in O_2 reaction pathways under electrochemical conditions.

The EDL at the metal/solution interface is characterized by excess charge density in the metal and counter charge of

* Corresponding author. Email address: will.medlin@colorado.edu

10.1021/jp045155y CCC: $30.25
Published on Web 03/15/2005

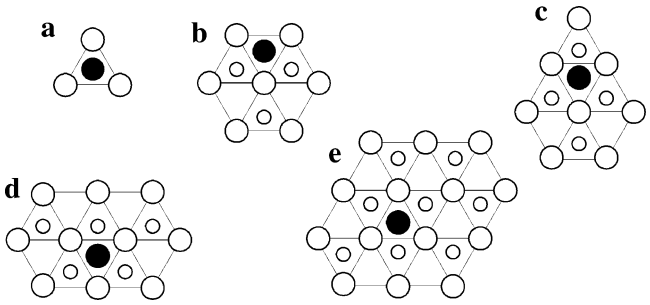

Figure 1. Cluster configurations used in this paper: (a) 3 Pt, (b) 10 Pt, (c) 12 Pt, (d) 15 Pt, and (e) 22 Pt. The large and small open circles correspond to first- and second-layer Pt atoms, respectively. The shaded circles correspond to the oxygen adsorption sites. In configuration c, the fcc hollow site used for the molecularly adsorbed oxygen state is the same as that shown here for the atomic oxygen state.

opposite sign in the solution, maintaining overall neutrality. The charge distribution and surface water dipole orientation are determined by the electrode potential. One technique used to model the effects of the EDL in theoretical studies is the application of homogeneous electric fields perpendicular to the interface.[42] This technique has been used in numerous DFT studies on finite clusters[43−45] but few periodic slab studies.[46]

To our knowledge, the effect of electric field strength on molecular oxygen adsorption and dissociation on Pt(111) has not been studied with either approach. In this paper, we report on theoretical calculations that describe the effect of applied electric fields on the interaction of various oxygen species with Pt(111). We also compare how the choice of model (cluster vs slab) affects the predicted influence of electric fields on oxygen adsorption and dissociation on Pt(111) and how those predictions compare with experimental data. Finally, we discuss implications of these results for the mechanism of oxygen reduction at fuel cathodes.

Methods

The finite-cluster calculations reported in this paper were performed with Amsterdam Density Functional (ADF),[47−49] which uses Slater-type basis sets. All calculations were performed with the standard double-ξ basis sets available in ADF and described in the cited references. Pt(111) clusters of 3−22 atoms were used, as shown in Figure 1. While the three-atom cluster returns comparatively inaccurate results, we include it to more clearly establish trends in the effects of cluster size. Frozen core approximations were employed, which included orbitals up to and including 4d for platinum and 1s for oxygen. The Pt−Pt bond distance was fixed at the experimental bulk distance of 2.772 Å.[50] Keeping the Pt−Pt bond distance fixed enables comparisons to be made with previously published studies on other adsorbate−substrate systems. The effect of surface relaxation as calculated with periodic slabs is discussed later in this paper. Most calculations were performed by use of the generalized gradient approximation with the BP86 functional.[51] In addition to BP86 calculations performed with the geometries listed in Table 1, selected calculations were performed with the PW91 functional[52] on the 12-atom clusters for comparison with periodic slab calculations. For those calculations that included electric fields, homogeneous fields of ±0.51 V/Å were applied perpendicularly to the surface. Additionally, the PW91 calculations also included fields of ±1.03 V/Å. Positive fields in this paper refer to positively charged surfaces.

Dacapo,[53,54] a total energy DFT program, was used to perform the periodic slab calculations reported in this paper. The basis set consists of plane-waves from ultrasoft pseudopotentials[55] with kinetic energy less than 25 Ry. Calculations were implemented with the PW91 functional. In all calculations, a (2×2) Pt(111) surface unit cell with four substrate layers was used. A $^1/_4$ ML adsorbate coverage was used for both atomic and molecular oxygen. Both frozen substrate calculations and relaxed substrate (with the bottom two layers frozen) calculations were executed. The frozen Pt−Pt distance was the same as in the finite-cluster calculations. The Brillouin zone was sampled by use of 18 k-points. Fermi populations were calculated at $k_BT = 0.1$ eV, while total energies were extrapolated to $k_BT = 0.0$ eV. Electric fields were applied in a manner similar to the finite-cluster calculations, but fields of ±0.5 V/Å and/or ±1 V/Å were applied.

Energies reported in this paper are electronic energies calculated with bare Pt and free O_2 as reference states. This can be written as

$$E = E_{\mathrm{Pt-O_x}} - E_{\mathrm{Pt}} - \frac{x}{2}E_{\mathrm{O_2}} \qquad (1)$$

where x is the number of oxygen atoms in the unit cell. Our baseline results (zero-field calculations) compare favorably to previous studies. The calculated binding energy for atomic oxygen in the face-centered cubic (fcc) hollow site with a relaxed substrate is −0.82 eV (−0.63 eV for the frozen substrate), close to −1.06 eV calculated with similar conditions.[5] We report the results of atomic oxygen only in the fcc hollow site. Our calculations, in agreement with previous studies,[3] show that adsorption in the fcc hollow is significantly more stable than in the other adsorption sites. Previous theoretical results indicate that molecular oxygen dissociates to form atomic oxygen in hexagonal close-packed (hcp) sites, which then diffuse to the more favorable fcc sites.[3] Our exploratory calculations show that electric field effects are similar between hcp and fcc sites. Likewise, we consider only the nonmagnetic molecular oxygen state, which binds to Pt(111) in the top-fcc-bridge (tfb) site with energy −0.44 eV (−0.23 eV unrelaxed), close to −0.6 eV as calculated by Sljivancanin and Hammer under similar conditions.[4] As previously noted, the magnetic and nonmagnetic oxygen states are nearly degenerate, but the nonmagnetic state is thought to be the dissociation precursor state.[3,8]

The dipole moments reported in this paper are calculated from geometry optimizations with zero electric field. These values are reported in units of debyes ($1\ \mathrm{D} = 3.33 \times 10^{-30}$ C·m). The polarizability values are calculated fit values from multiple linear regression analysis. The values reported (in units of cubic angstroms) are the true fit values (in units of coulomb^2 meter^2 joule^{-1}) divided by $4\pi\epsilon_o$, where ϵ_o is the permittivity of vacuum.

Results

(A) Finite Cluster Calculations: (1) Atomic Oxygen Adsorption. Preliminary calculations focused on the effect of electric field strength on the adsorption energy for atomic oxygen. Here, as elsewhere, the range of electric field strengths considered is based on the estimated electric field in the EDL. If an inner-layer thickness of 3 Å is assumed, a ±0.5 V/Å electric field corresponds to an electrode potential of approximately ±1.5 V from the potential of zero charge,[56] consistent with the range of voltages present in fuel cells. Figure 2 shows the effect of the electric field on the binding energy of an O atom adsorbed in the fcc hollow of a 10-atom Pt cluster. The negative field stabilizes the interaction while the positive field has the opposite effect. The relationship between the change in energy and the electric field can be approximated by

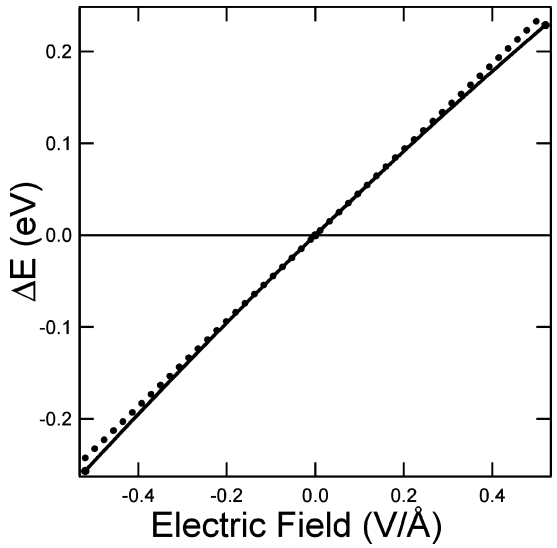

Figure 2. Binding energy shifts for atomic oxygen on a 10-atom Pt(111) cluster predicted by first-order Stark effect (···) and calculated from DFT (—). The DFT data follow the Stark effect data very closely, suggesting that the large binding energy shifts are almost entirely due to changes in the stability of the static dipole moment.

the first-order Stark effect, representing the (de)stabilization of the static dipole moment, and is given by

$$\Delta E = -\mu F \tag{2}$$

where ΔE is the binding energy change due to the imposed electric field, μ is the zero-field dipole moment, and F is the electric field. The dipole moments reported are the net dipole moments (adsorbate−substrate minus substrate) induced by adsorption in the direction perpendicular to the surface. The electrostatic interaction between the dipoles and the parallel electric fields alter the binding energies in accordance to eq 2. In our sign convention, the dipole moment of oxygen (an electron-withdrawing species) is negative. Figure 2 clearly shows that the effect of the field matches this relationship very well, indicating that the electric field effects on binding energy are primarily through interaction with the large adsorbate dipole (2.26 D). These data are consistent with previously published studies.[43−45]

Wasileski and Weaver[57] noted that the electric field effect as calculated by clusters is only qualitative and that the dipole moment changes with cluster geometry. This dependence for the Pt(111) clusters of various geometries and sizes is observed in Figure 3 to be of dramatic importance. The dipole moment decreases markedly with the number of platinum atoms. In contrast, the binding energy of O/Pt(111) does not change significantly with cluster size for >10 Pt atoms. [The observed small-scale binding energy fluctuations with cluster size are not unusual and have been observed previously for O, H, and OH on Ag(111).[44]] Whereas the binding energy of atomic oxygen converges to a steady value for clusters containing 10 Pt atoms or more, the dipole strength does not. Thus, the convergence of the binding energy does not imply a convergence of the dipole strength. As demonstrated below, the failure of small cluster calculations to capture the dipole moment for molecular oxygen has profound implications for assessing the true effect of electric field application. To illustrate how binding energy shifts resulting from imposition of electric fields depend on cluster size, the predicted change in binding energy is plotted versus cluster size for the application of a 0.51 V/Å electric field in Figure 4. The plotted data give no indication that the dipole

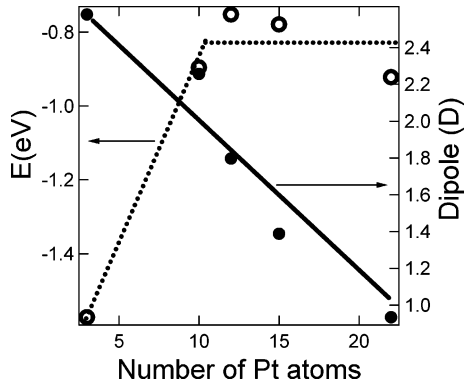

Figure 3. Cluster size dependence on binding energy (○) and dipole moment (●). The binding energy is stable on clusters with >10 Pt atoms, whereas the dipole moment decreases nearly linearly with cluster size.

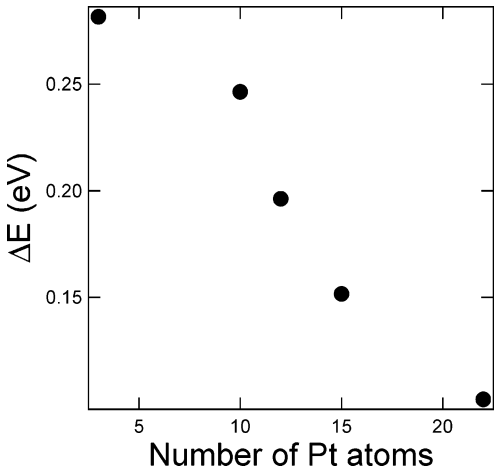

Figure 4. Predicted binding energy shift for atomic oxygen on Pt(111) clusters with an applied electric field of 0.51 V/Å. The binding energy is calculated from the first-order Stark effect. The plot follows the same trend as Figure 2, with the smaller clusters affected most severely by the electric field.

strength is converging with increasing cluster size; it is possible that significantly more than 22 atoms are required to achieve true convergence. The necessity of using large clusters to successfully model the adsorbate dipole moment suggests that slab calculations may be necessary for even roughly accurate determinations of electric field effects.

(2) Molecular Oxygen Adsorption and Dissociation. The adsorbed oxygen dissociation precursor (the nonmagnetic state bound in the top-fcc-bridge site) and transition-state complex were also investigated on 12-atom Pt clusters. The linearity of the data in Figure 5 shows that the first-order Stark effect dominates for the molecular oxygen calculations (dipole 2.92 D) as it does for the atomic oxygen calculations (1.99 D), but the O_2 calculations clearly exhibit a curvature not seen in the atomic oxygen calculations. This curvature is attributable to the second-order Stark effect, the stabilization of the energy due to an induced dipole moment, given by

$$\Delta E = -\alpha F^2 \tag{3}$$

where α is the polarizability of the surface structure. The polarizability of adsorbed molecular oxygen is estimated to be 1.31 Å^3 by fitting α to the curve in Figure 5. As was observed for atomic oxygen, the magnitude of the binding energy shifts caused by electric field application is highly dependent on cluster

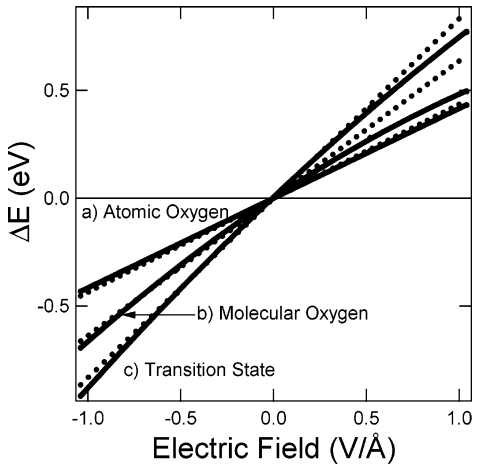

Figure 5. Binding energy shifts for (a) atomic oxygen, (b) molecular oxygen, and (c) the dissociation transition state on a 12-atom Pt(111) cluster. Predicted first-order Stark effect energy shifts (···) and calculated binding energy shifts (—) are shown. The calculated binding energy shifts of the molecular states exhibit noticeable deviation from predicted values, suggesting that the induced dipole stabilization effect is significant.

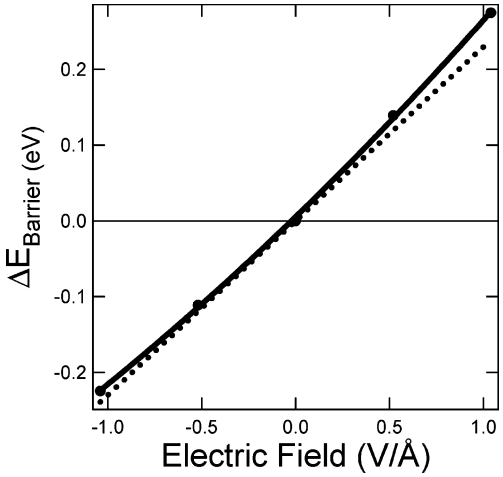

Figure 6. Dissociation energy barrier shifts on a 12-atom Pt(111) cluster. The energy is calculated by subtracting the precursor energy from the transition-state energy. Predicted first-order Stark effect energy shifts (···) and calculated energy shifts (—) are shown.

size, which again can be attributed to large variation in computed dipole strength. This point will be discussed in greater detail below.

To understand how electric fields affect the dissociation pathway of molecular oxygen, it is important to determine how the kinetics of the reaction change in the presence of an electric field. For this reason, we have computed the effect of applied electric fields on the transition state for O_2 dissociation (dipole, 4.01 D; fitted α, 0.95 Å^3). To reiterate, previous groups have concluded that the molecular precursor state adsorbed in the tfb site dissociates to atomic oxygen in two hcp sites.[3,8] Our own transition-state calculations following this pathway indicate the dissociation barrier to be 0.44 eV at zero electric field. Experimentally, the dissociation barrier was estimated from time-resolved EEL spectra to be 0.29 eV.[8] Previous DFT periodic slab studies have estimated the barriers to be 0.6 eV[4] and 0.9 eV.[2] Figures 5 and 6 show the effect of electric field application on the transition-state energy and dissociation barrier, respectively. The change in dissociation barrier energy is calculated by subtracting the energy change in the molecular oxygen state from the energy change in the transition state.

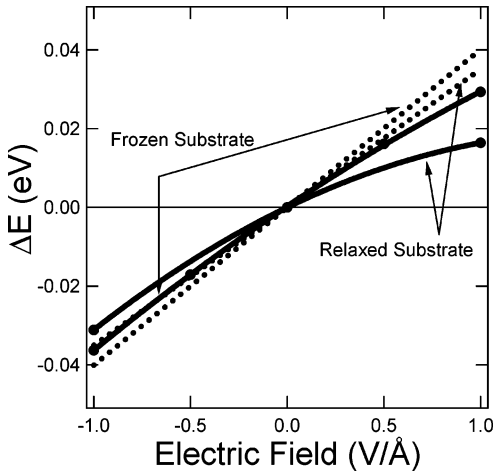

Figure 7. Binding energy shifts for atomic oxygen on Pt(111) slabs: DFT data (—) and first-order Stark effect data (···). The relaxed substrate data exhibits significantly more curvature and an overall smaller electric field effect than the frozen substrate data. The binding energy shifts of both substrate types are an order of magnitude lower than those of atomic oxygen on both the 10- and 12-atom Pt(111) clusters.

Although the electric field has a rather large effect on the transition-state energy, the effect on the molecular oxygen adsorption is nearly as large, so that the overall effect is modest.

These cluster calculations would appear to indicate that the applied electric field has a large effect on the interaction of oxygen with Pt(111). For the 12-atom clusters used here—which are similar in size and geometry to those used in previous studies—the deviations from the zero-field binding energies are quite large, accompanied by a smaller but notable effect on the dissociation barrier. From these data, one would predict that the stability of oxygen species for the positive electric fields, which correspond to cathodes, would be drastically reduced, resulting in less thermodynamically favorable oxygen interactions with Pt and likely in lower surface coverages. The activation energy would be moderately increased, leading to a slower dissociation rate. The slower O_2 dissociation kinetics may offer an explanation for the relatively slow rates (and large overpotentials) associated with oxygen reduction under electrochemical conditions. They may also result in the proposed difference in oxygen reduction mechanisms observed in gas-phase reactions and electrochemical reactions on platinum catalysts. However, periodic slab calculations, discussed below, suggest qualitatively different results.

(B) Periodic Calculations: (1) Atomic Oxygen Adsorption. Geometry optimizations for atomic oxygen on Pt(111) slabs were conducted as a function of electric field strength. As in the cluster calculations, the fcc hollow was identified as the most stable adsorption site; results discussed here will therefore focus on binding in that site. Figure 7 shows the effect of application of a uniform electric field on the binding energy of atomic oxygen on a frozen Pt(111) slab. These slab results reveal a noticeably different effect of electric field application as compared to small cluster calculations (Figure 2). Adsorbed atomic oxygen on the frozen Pt(111) slab with four substrate layers has a significantly smaller dipole moment (0.19 D) than on the clusters. The frozen substrate plot, as seen in Figure 7, has a small but noticeable curvature, suggesting the polarizability is small (estimated to be 0.049 Å^3 by fitting α to the data). Surface relaxation lowers the dipole moment to 0.17 D and therefore results in smaller binding energy shifts compared to the frozen substrate. We attribute this difference to the fact that

the oxygen atom is ca. 0.1 Å closer to the surface Pt atoms forming the hollow site, although it is ca. 0.2 Å farther away from the bulk. Relaxation decreases the distance between the oxygen atom charge and the platinum image charge, therefore decreasing the dipole strength. The curvature is noticeably larger, with a fitted α of 0.11 Å^3. (We note that dipole moments values obtained from fits of adsorption energy vs electric field plots were systematically less than the zero-field dipole moments by 10−20% for atomic and molecular oxygen; similar error may be expected in the polarizabilities.) While the surface relaxed calculations more accurately represent the physics of the surface, the frozen surface calculations can semiquantitatively determine the effects of an electric field. Dipole moments estimated by use of the Helmholtz equation from previous Kelvin probe studies (0.10 D[58] and 0.18 D[59]) are close to our calculated dipole moments. These experimental results, combined with the size dependence on dipole moment in cluster calculations, indicate that more accurate binding energy shifts are obtained from the periodic slab calculations than cluster calculations. Furthermore, these more accurate slab calculations indicate that the effect of an applied electric field on the O adsorption energy is relatively small, in contrast to what one finds with cluster calculations.

Various attempts were made to determine whether, by changing the computational parameters, it was possible to observe larger dipole moments in the slab calculations. The zero-field dipole moments of adsorbed atomic oxygen on frozen two- and three-layer slabs were both calculated to be 0.18 D, indicating no systematic size dependence. Thus, use of even a relatively small number of Pt atoms in the slab unit cell yields a fairly accurate dipole moment, in contrast to cluster calculations. Exploratory calculations were also performed at lower coverage conditions to determine whether lateral adsorbate interactions could be partly responsible for decreasing the dipole moment. The dipole moment of atomic oxygen on a 3×3 unit cell with three substrate layers is 0.22 D, indicating that adsorbate−adsorbate repulsion may slightly decrease the effects of the electric field, but not to a degree sufficient to explain the deviations between the cluster and slab results.

(2) Molecular Oxygen Adsorption and Dissociation. As with the cluster calculations, we only considered the nonmagnetic molecular oxygen state adsorbed in the tfb site. The effect of surface relaxation on the height of the oxygen atoms above the surface is similar to that in the atomic oxygen calculations. In agreement with the results for atomic oxygen, the effect of applied electric fields on binding energy is computed to be much weaker in the slab calculations compared to the cluster calculations. Figure 8 shows the binding energy shifts for molecular oxygen bound to both frozen and relaxed substrates. Both substrate results display significant curvature, with fitted α values of 0.58 Å^3 (frozen) and 0.64 Å^3 (relaxed). Our calculated dipole moments of 0.39 D (frozen) and 0.36 D (relaxed) compare very favorably with the experimental value of 0.36 D estimated from work function data.[14] The experimental value, however, does not distinguish between the magnetic and nonmagnetic molecularly adsorbed states. (We calculated the dipole moment of the magnetic state on a relaxed substrate to be 0.26 D.) Despite this uncertainty, the binding energy shifts in the slab calculations are clearly more accurate than the cluster calculations when one considers the zero-field dipole moment of O_2 bound to the 12-atom cluster is 2.92 D.

The transition state (TS) structure, in comparison to the adsorbed oxygen states, is greatly affected by the electric field, as shown in Figure 9. The zero-field dipole moment of the TS on a frozen substrate was calculated to be 1.22 D, significantly larger than molecular oxygen. The fitted α of 0.60 Å^3, however, is very close to the molecular oxygen value. Although the dipole moment is much less than that calculated with the 12-atom cluster, the difference between the TS and molecular structures in both models is not nearly as large. As such, the energy change of the activation barrier due to the electric field when calculated with the slab, as shown in Figure 9, is similar to that calculated with the cluster. The relatively good agreement between slab and cluster calculations for the dissociation barrier may be the result of a cancellation of errors in the cluster calculations but is likely an anomalous observation not valid for the effect of electric fields on surface reactions in general. In the slab calculations, an applied electric field of 0.5 V/Å results in an increase in the dissociation barrier of just over 0.1 eV. While modest, this increase is sufficient to significantly slow the dissociation kinetics and may be sizable enough to cause another dissociation pathway to be favored under electrochemical conditions.

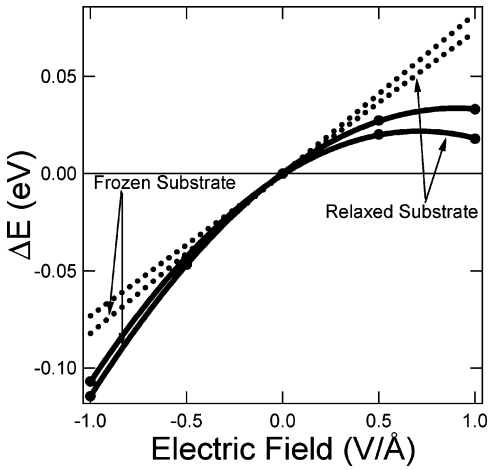

Figure 8. Binding energy shifts for molecular oxygen on Pt(111) slabs: DFT data (—) and first-order Stark effect data (···). Both substrate curves exhibit substantial curvature, suggesting that the electric field induces a significant stabilizing dipole moment in addition to the static dipole moment. The binding energy shifts are significantly smaller than those on the 12-atom Pt(111) cluster. In the positive electric field, the binding energy shift is minimal on the relaxed substrate.

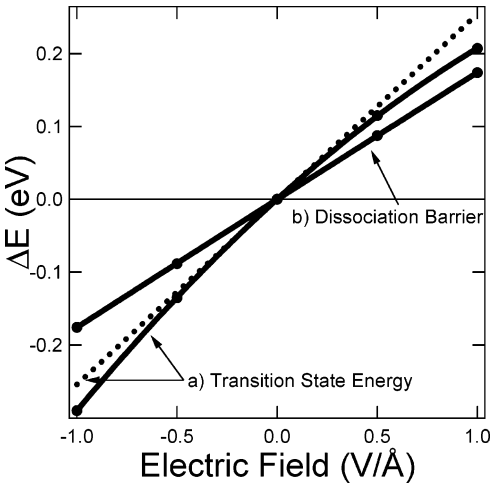

Figure 9. Frozen substrate calculations for (a) binding energy shifts in transition state (TS) oxygen and (b) dissociation barrier shifts: DFT data (—) and first-order Stark effect data (···). The TS shifts are significantly smaller than on the 12-atom cluster, but dissociation barrier shifts are relatively close.

Implications for the Oxygen Reduction Reaction at the Cathode. With the results presented in this paper, we can better understand how applying an electric field influences oxygen dissociation. Since we are interested in oxygen reduction at fuel cell cathodes, we will only consider positive electric fields in this discussion. In cluster calculations, the large increase in binding energy due to the applied electric fields for the three oxygen states considered here—molecular, atomic, and dissociation transition state—suggests that the destabilization of the oxygen species could result in a different oxygen reduction mechanism in the EDL at the cathode. The slab calculations suggest a much smaller electric field effect on the adsorption strengths of oxygen atoms; however, the dipole moment of the transition state is large enough that the dissociation kinetics could be altered. Whether this electrostatic effect alone can account for a new mechanism in the EDL is questionable. In addition to electrostatically destabilizing the oxygen−platinum interaction, the field may indirectly alter the reaction mechanism by influencing the stability of other reaction intermediates or spectator species, particularly H_2O. This report clearly shows that cluster calculations overpredict the dipole strength and may be insufficient for assessing the magnitude of the electric field effects on the kinetics and thermodynamics of adsorbate reactions on electrodes. Slab calculations must be used to assess how EDL physics alter reaction pathways observed in a vacuum.

Conclusions

The adsorption of both atomic and molecular oxygen on Pt(111) is stabilized by negative electric fields and destabilized by positive electric fields. This energy change due to the electric field is primarily a result of the (de)stabilization of the static dipole moment. While the qualitative effect of these electric fields is apparent from cluster calculations, the magnitude of the effect is drastically overpredicted. The data clearly demonstrate that the static dipole moment calculated with the cluster model is a strong function of the size of the cluster. Slab calculations have been found to predict smaller adsorbate dipole moments and reduced electric field effects on binding energy; these results are in good agreement with available experimental data. Surface relaxation of the slabs, which is not accounted for in cluster calculations, lowers the static dipole moment, albeit not significantly enough to alter the conclusions reached by use of either calculation method. In the slab calculations, there is clearly a large second-order energy correction due to a significant induced dipole moment due to the polarizability of adsorbed oxygen, particularly for molecular oxygen.

By use of the more accurate slab calculation results, it has been found that the adsorption energies of atomic and molecular oxygen on Pt(111) are only slightly affected by the imposition of large electric fields. A modest shift in the oxygen dissociation barrier of ca. 0.1 eV is predicted for the application of a positive electric field of 0.5 V/Å. These results suggest that the thermodynamics of O_2 adsorption and dissociation are not substantially affected by the presence of an electric field but that the kinetics may be altered. Moreover, the results presented here suggest that destabilization of adsorbate dipoles may play some role in controlling the mechanism of O_2 reduction at fuel cell cathodes, but other factors (including the presence of coadsorbates, an acidic environment, and H_2O) that affect the physics of electrochemical environments must be investigated to arrive at a more complete understanding.

Acknowledgment. This research was supported in part by a grant of computer time from the Partnership for Advanced Computational Infrastructure (PACI), a program of the National Science Foundation (NSF) Directorate for Computer and Information Science and Engineering (CISE).

References and Notes

(1) Bocquet, M. L.; Cerda, J.; Sautet, P. *Phys. Rev. B* **1999**, *59*, 15437.
(2) Eichler, A.; Hafner, J. *Phys. Rev. Lett.* **1997**, *79*, 4481.
(3) Eichler, A.; Mittendorfer, F.; Hafner, J. *Phys. Rev. B* **2000**, *62*, 4744.
(4) Sljivancanin, Z.; Hammer, B. *Surf. Sci.* **2002**, *515*, 235.
(5) Watwe, R. M.; Cortright, R. D.; Mavrikakis, M.; Norskov, J. K.; Dumesic, J. A. *J. Chem. Phys.* **2001**, *114*, 4663.
(6) Steininger, H.; Lehwald, S.; Ibach, H. *Surf. Sci.* **1982**, *123*, 1.
(7) Avery, N. R. *Chem. Phys. Lett.* **1983**, *96*, 371.
(8) Nolan, P. D.; Lutz, B. R.; Tanaka, P. L.; Davis, J. E.; Mullins, C. B. *J. Chem. Phys.* **1999**, *111*, 3696.
(9) Nolan, P. D.; Lutz, B. R.; Tanaka, P. L.; Davis, J. E.; Mullins, C. B. *Phys. Rev. Lett.* **1998**, *81*, 3179.
(10) Outka, D. A.; Stohr, J.; Jark, W.; Stevens, P.; Solomon, J.; Madix, R. J. *Phys. Rev. B* **1987**, *35*, 4119.
(11) Stohr, J.; Gland, J. L.; Eberhardt, W.; Outka, D.; Madix, R. J.; Sette, F.; Koestner, R. J.; Doebler, U. *Phys. Rev. Lett.* **1983**, *51*, 2414.
(12) Grimblot, J.; Luntz, A. C.; Fowler, D. E. *J. Electron Spectrosc. Relat. Phenom.* **1990**, *52*, 161.
(13) Gland, J. L.; Korchak, V. N. *Surf. Sci.* **1978**, *75*, 733.
(14) Gland, J. L.; Sexton, B. A.; Fisher, G. B. *Surf. Sci.* **1980**, *95*, 587.
(15) Gland, J. L. *Surf. Sci.* **1980**, *93*, 487.
(16) Luntz, A. C.; Grimblot, J.; Fowler, D. E. *Phys. Rev. B* **1989**, *39*, 12903.
(17) Gland, J. L.; Fisher, G. B.; Kollin, E. B. *J. Catal.* **1982**, *77*, 263.
(18) Creighton, J. R.; White, J. M. *Surf. Sci.* **1982**, *122*, L648.
(19) Fisher, G. B.; Gland, J. L.; Schmieg, S. J. *J. Vac. Sci. Technol.* **1982**, *20*, 518.
(20) Ogle, K. M.; Creighton, J. R.; Luftman, H. S.; White, J. M. *J. Chem. Phys.* **1983**, *78*, 5839.
(21) Ogle, K. M.; White, J. M. *Surf. Sci.* **1984**, *139*, 43.
(22) Ogle, K. M.; White, J. M. *Surf. Sci.* **1986**, *169*, 425.
(23) Mitchell, G. E.; Akhter, S.; White, J. M. *Surf. Sci.* **1986**, *166*, 283.
(24) Mitchell, G. E.; Akhter, S.; White, J. M. *J. Vac. Sci. Technol. A* **1986**, *4*, 1472.
(25) Anton, A. B.; Cadogan, D. C. *Surf. Sci.* **1990**, *239*, L548.
(26) Hellsing, B.; Kasemo, B.; Zhdanov, V. P. *J. Catal.* **1991**, *132*, 210.
(27) Anton, A. B.; Cadogan, D. C. *J. Vac. Sci. Technol., A: Vac. Surf. Films* **1991**, *9*, 1890.
(28) Capitano, A. T.; Gabelnick, A. M.; Gland, J. L. *Surf. Sci.* **1999**, *419*, 104.
(29) Michaelides, A.; Hu, P. *J. Am. Chem. Soc.* **2001**, *123*, 4235.
(30) Michaelides, A.; Hu, P. *J. Chem. Phys.* **2001**, *114*, 513.
(31) Nagasaka, M.; Kondoh, H.; Amemiya, K.; Nambu, A.; Nakai, I.; Shimada, T.; Ohta, T. *J. Chem. Phys.* **2003**, *119*, 9233.
(32) Stamenkovic, V.; Schmidt, T. J.; Ross, P. N.; Markovic, N. M. *J. Phys. Chem. B* **2002**, *106*, 11970.
(33) Paulus, U. A.; Wokaun, A.; Scherer, G. G.; Schmidt, T. J.; Stamenkovic, V.; Markovic, N. M.; Ross, P. N. *Electrochim. Acta* **2002**, *47*, 3787.
(34) Paulus, U. A.; Wokaun, A.; Scherer, G. G.; Schmidt, T. J.; Stamenkovic, V.; Radmilovic, V.; Markovic, N. M.; Ross, P. N. *J. Phys. Chem. B* **2002**, *106*, 4181.
(35) Sepa, D. B.; Vojnovic, M. V.; Damjanovic, A. *Electrochim. Acta* **1981**, *26*, 781.
(36) Sepa, D. B.; Vojnovic, M. V.; Vracar, L. M.; Damjanovic, A. *Electrochim. Acta* **1987**, *32*, 129.
(37) Ghoneim, M. M.; Clouser, S.; Yeager, E. *J. Electrochem. Soc.* **1985**, *132*, 1160.
(38) Yeager, E.; Razaq, M.; Gervasio, D.; Razak, A.; Tryk, A. D. The electrolyte factor in O_2 reduction electrocatalysis. Proceedings, Structural Effects on Electrocatalysis and Oxygen Electrochemistry, 1991, Cleveland, OH. Scherson, D., Tryk, M., Daroux, M., Xing, X., Eds.; Electrochemical Society Proceedings, Vol. 92-11, ECS: Pennington, NJ, 1992.
(39) Anderson, A. B.; Albu, T. V. *J. Electrochem. Soc.* **2000**, *147*, 4229.
(40) Sidik, R. A.; Anderson, A. B. *J. Electroanal. Chem.* **2002**, *528*, 69.
(41) Li, T.; Balbuena, P. B. *Chem. Phys. Lett.* **2003**, *367*, 439.
(42) Nazmutdinov, R. R.; Shapnik, M. S. *Electrochim. Acta* **1996**, *41*, 2253.
(43) Koper, M. T. M.; van Santen, R. A.; Wasileski, S. A.; Weaver, M. J. *J. Chem. Phys.* **2000**, *113*, 4392.

(44) Koper, M. T. M.; van Santen, R. A. *J. Electroanal. Chem.* **1999**, *472*, 126.
(45) Wasileski, S. A.; Koper, M. T. M.; Weaver, M. J. *J. Chem. Phys.* **2001**, *115*, 8193.
(46) Liu, P.; Logadottir, A.; Norskov, J. K. *Electrochim. Acta* **2003**, *48*, 3731.
(47) Amsterdam Density Functional; ADF2002.03 ed.; Vrije Universiteit, Department of Theoretical Chemistry, Amsterdam, 2002.
(48) Baerends, E. J.; Ellis, D. E.; Ros, P. *Chem. Phys.* **1973**, *2*, 41
(49) Velde, G. T.; Bickelhaupt, F. M.; Baerends, E. J.; Guerra, C. F.; Van Gisbergen, S. J. A.; Snijders, J. G.; Ziegler, T. *J. Comput. Chem.* **2001**, *22*, 931.
(50) Kittel, C. *Introduction to Solid State Physics*, seventh ed.; John Wiley & Sons: New York, 1996.
(51) Perdew, J. P. *Phys. Rev. B* **1986**, *33*, 8822.
(52) Perdew, J. P.; Chevary, J. A.; Vosko, S. H.; Jackson, K. A.; Pederson, M. R.; Singh, D. J.; Fiolhais, C. *Phys. Rev. B* **1992**, *46*, 6671.
(53) Hammer, B.; Hansen, L. B.; Norskov, J. K. *Phys. Rev. B* **1999**, *59*, 7413.
(54) http://www.fysik.dtu.dk/campos/Dacapo/.Dacapo.
(55) Vanderbilt, D. *Phys. Rev. B* **1990**, *41*, 7892.
(56) Wasileski, S. A.; Weaver, M. J.; Koper, M. T. M. *J. Electroanal. Chem.* **2001**, *500*, 344.
(57) Wasileski, S. A.; Weaver, M. J. *J. Phys. Chem. B* **2002**, *106*, 4782.
(58) Derry, G. N.; Ross, P. N. *J. Chem. Phys.* **1985**, *82*, 2772.
(59) Hohenegger, M.; Bechtold, E.; Schennach, R. *Surf. Sci.* **1998**, *413*, 184.